$$E_{aM}/E_d=\frac{2\sqrt{3}}{\pi}=1.1,\quad E_{bM}/E_d=\frac{\sqrt{3}}{2}=0.866,$$
$$E_{cM}/E_d=1.0 \qquad (22)$$

Fig. 11 shows the variation of the principal components of the new PWM waveform to the modulating index M. Fig. 12 represents the characteristics of the DC output voltage as the AC to DC converter by the new PWM control. The fundamental component of the PWM waveform and the DC average voltage are linearly controlled by the modulating index M. The maximum effective value is about 1.1 times of the fundamental component. The high total power factor (PF) near the unity will be obtained over the wide range of the output control because of the unity fundamental power factor $(PF)_1$ by using the filters to suppress the switching harmonics.

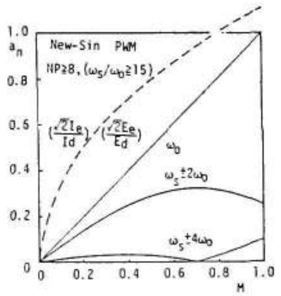

Fig. 11. New PWM characteristics for modulating index M..

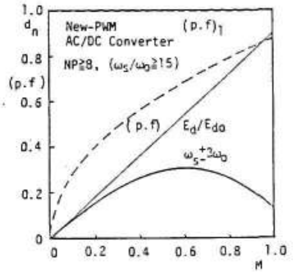

Fig. 12. DC output characteristics of new PWM.

5. Experimental Results

5.1 Voltage source PWM inverter

The experimental results are obtained by the 3.5 kVA transistor inverter. Fig. 13 shows the resulting oscillograms of the three kinds of PWM output voltage (upper) and current (lower) waveforms and it's spectrums with the theoretical value for comparisons, which are operated in the same condition as next ; [$E_a=200$ V, $f_a=60$ Hz (three-phase AC power line), $f_o=60$ Hz (output frequency) and $Z_L=15.5\ \Omega$, $(PF)_L=0.8$ (load power factor)]. Fig. 13 (i) and (ii) are the results for the new PWM of $NP=16$ and $NP=8$ respectively. Fig. 13 (iii) is for the conventional PWM waveform of $NP=15$. As may be prospected from the voltage spectrum, the current waveform of the new PWM for $NP=16$ (i) is very close to a sinusoidal one compared with that of the conventional PWM for $NP=15$ (iii). The output waveform of the new PWM for $NP=8$ (ii) is similar to that of the conventional one for $NP=15$ (iii). Fig. 14 shows the comparisons of the output characteristics for the new and conventioal PWM obtained under the same operating conditions. The results are considerably agree with the theoretical one shown in Fig. 9. It can be seen that the efficiency is affected by the number of the PWM pulses. Fig. 15 shows the experimental comparisons between the new PWM ($NP=8$) and the conventional PWM ($NP=15$) for the same switching times ($NS=15$). The higher

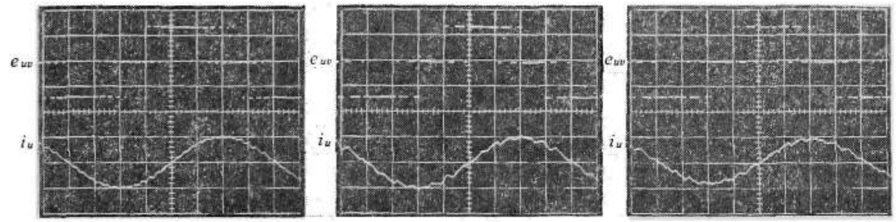

(a) Waveforms-volt/curr. [$(PF)_L=0.8$ lagging] Waveforms-volt/curr. [$(PF)_L=0.8$ lagging] Waveforms-volt/curr. [$(PF)_L=0.8$ lagging]

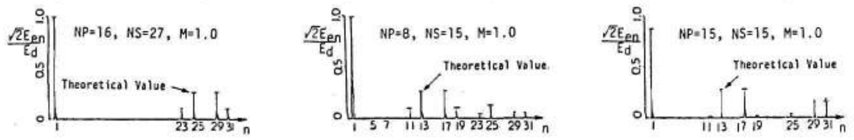

(b) Spectrum-volt (e_{uv}). (i) New-PWM Spectrum-volt (e_{uv}). (ii) New-PWM Spectrum-volt (e_{uv}). (iii) Conv.-PWM

Fig. 13. Oscillograms of PWM output waveforms (upper : 270 V/div, lower : 10 A/div) and it's spectrums of voltage source transistor inverter.

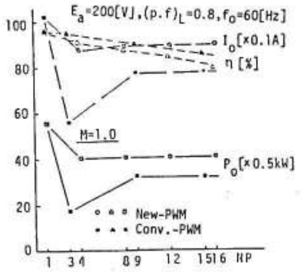

Fig. 14. Comparisons of resulting output characteristics between new PWM and convenional PWM.

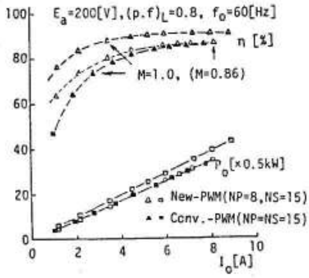

Fig. 15. Comparisons of efficiences and output power between two PWMs with similar output spectrums.

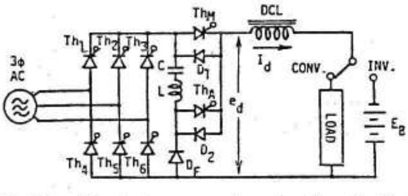

Fig. 16. Thyristor converter circuit suitable for new PWM scheme.

output and efficiency can be obtained for the new PWM inverter which may be caused by the difference of the output gain for the same modulating index (M =1.0). The efficiency of the new PWM inverter for the same output gain as the conventional one is also shown in the figure for the comparison.

The successful driving by the new PWM inverter is confirmed for the speed control of an induction motor.

5.2 Current source type converter

Fig. 16 shows the AC to DC converter constructed by the thyristor bridge with the commutation circuit suitable for the new PWM technique(15). The bidirectional power conversion is easily performed only by changing the gate pulse sequence to the thyristors, which is a significant feature of the current fed converter. The gate pulse patterns of the thyristor bribge circuit are shown in Fig. 4 (b) and the gate pulse for the commutation circuit is obtained from the P_3. Fig. 17 shows (a) the oscillogram of the three-phase PWM current and the voltage waveforms, and (b) the spectrum of the current obtained by this circuit under the operating condition as next ; [E_a=200 V, f_a=60 Hz (three-phase power line), I_d=10 A (DC current) and NP=8, M=0.5]. The inverting operation is performed successfully by the same circuit as the converting operation. It is verified that the sinusoidal PWM current waveform can be obtained for the current source power converter too. The driving characteristics of the DC motor by this circuit is shown in Fig. 18. The rating of the DC motor are as follows ; [P_r=1.5 kW, N_r=1,750 rpm, E_{dr}=180 V, I_{dr}=9.3 A]. The DC motor can be smoothly controlled and the higher efficiency η can be obtained. If the AC filters to eliminate the higher harmonics of the PWM current is used, the higher power factor (PF) will be obtained, because the fundamental power factor $(PF)_1$ holds about unity over the wide range of the output control as shown. On the other hand, the toal power factor of the conventional phase controlled converter can not be improved

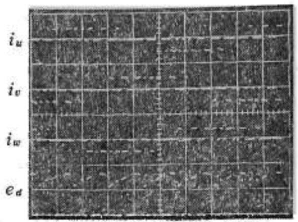

(a) Waveforms-curr./volt.

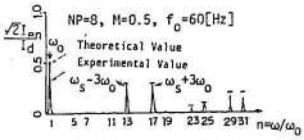

(b) Spectrum-curr(i_u).

Fig. 17. Oscillogram (160 V / div, 20 A/div) and it's spectrum of PWM output.

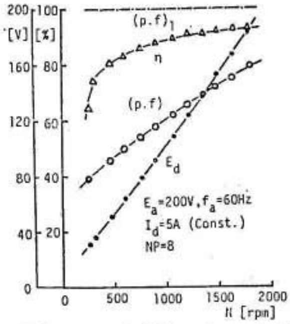

Fig. 18. DC motor driving characteristics by new PWM Converter.